

Density-driven Natural Convection in Dual Layered and Anisotropic Porous Media with Application for CO₂ Injection Projects

R. Farajzadeh, F. Farshbaf Zinati, P.L.J. Zitha and J. Bruining

Department of Geotechnology Delft University of Technology, The Netherlands

1. Introduction

The growing concern over global warming has increased the impetus to examine various ways to reduce the emission of greenhouse gases into the atmosphere. The increase in the concentration of CO₂ in the atmosphere is of particular concern. A viable technique consists in storing CO₂ in geological formations, for example, in depleted oil and gas reservoirs, deep saline aquifers and coal beds. The geological storage of CO₂ is mostly accomplished by injecting it in dense form into a deep porous rock formation containing mainly water and small amounts of oil. The quantification of CO₂ dissolution in those subsurface fluids is of paramount importance in CO₂ sequestration projects.

When CO₂ is injected into the porous formation, initially the injected CO₂ accumulates under the cap rock and subsequently dissolves into the formation liquid by molecular diffusion [1]. The densities of the water-CO₂ and oil-CO₂ solutions increase with CO₂ concentration [2,3]. As a result, the density of liquid increases and eventually CO₂-liquid interface becomes unstable. For favorable conditions, natural convection occurs and enhances the mass transfer of CO₂ [4-6].

In practice porous media are anisotropic, often with a horizontal permeability that is much larger than the vertical permeability. Moreover the subsurface is heterogeneous, with the main characteristic that they have a layered structure. In many situations of practical interest areal heterogeneity is ignored. Most of the papers dealing with natural convection in heterogeneous and/or anisotropic media are concerned with an imposed temperature or concentration difference between the top and bottom of the considered formation. Moreover these studies are limited to steady state behavior (e.g. Refs. 7-16). Both analytical and numerical aspects are considered. To our knowledge there are no numerical studies on the transient behavior of natural convection in either anisotropic or layered systems. Ennis King et al. [17] consider the onset of convection of a contaminant (solid or dissolved gas) in an anisotropic medium from both a normal mode analysis and an energy analysis. They find the critical wave length and critical time at the onset of natural convection. They find that a decreasing vertical permeability counteracts natural convection and increases the time at which natural convection occurs. They distinguish two regimes. In one regime the diffusive transport of contaminant has been travelling a distance of the order of the layer thickness before the onset of convection occurs. In the other regime the diffusive layer is much thinner. For both cases the dependence of the critical Rayleigh number on the anisotropy ratio is given in their paper. Kimura and Okajima [9] examine the effect of anisotropy in a porous cavity and conclude that when permeability ratio, ϑ , tends to zero, heat transfer across the cavity approaches the conductive state and the convective velocity, which is primarily in the vertical direction, scales with the product of the Rayleigh number and permeability ratio. When ϑ tends to infinity the convective velocity scales with Ra and it is independent of permeability ratio. McKibben et al. [8,12,13] consider the situation of periodic porous media. The main conclusion of the paper is that for a small number of layers, the convection can be confined to one or a few layers and that for many layers the situation may approach the behavior of a single homogeneous layer. They also found that very small permeability at the top layer is required to force the convection to occur mainly in the bottom layer and as can be expected most of the flow takes place in the high permeable layer. Vasseur and Wang [15] study the steady state natural convection heat transfer in a porous medium with multiple vertical partitions. They found that the maximum heat transfer happens when the system is heated from bottom. Leong and Lai [14] considered a layered porous medium heated from the sides, for different layering configurations. They stated that in principle the lumped system approach is generally applicable to tall porous cavities, although the method is less successful for shallow cavities. Tyvand [10] considers the effects of cross-flow, anisotropic permeability

and velocity dependent diffusion coefficients. However his study is limited to steady state cases.

In our previous paper [18] we investigated transient natural convection in a 2-D slab, containing an isotropic homogeneous porous medium saturated with water. The top of the slab was exposed to CO₂, such that the top layer contained a solution saturated with carbon dioxide. An initial perturbation was imposed to study the behavior of the ensuing fingering. We found that natural convection increases with increasing Rayleigh number, which depends both on the characteristics of the porous medium, mainly the permeability, and the fluid properties. With increasing aspect ratio, the time to see the beginning of the natural convection decreases. The simulation results show that the non-linear behavior of the flow is strongly dependent on the Rayleigh number. However, as time proceeds the number of the fingers decreases due to the decreasing effect of natural convection. Initially, the CO₂ front moves proportional to the square root of time for different Rayleigh numbers and then the relationship becomes linear. The transition time at which the switching occurs decreases with increasing Rayleigh number. This paper extends our previous work by considering dual layered and/or anisotropic porous media.

Section 2 describes the set-up that we have used to measure CO₂ mass-transfer between into a two-layered porous medium initially saturated with water. We show results both for a high permeable layer on top and a low permeable layer on top. Section 3 presents the physical model and state the ensuing model equations. It also presents the numerical model. The results and discussion in section 4 gives concentration profile for four cases, i.e. high permeable layer or low permeable layer on top and for the isotropic and anisotropic case. In all cases we start with a wavy perturbation on the top. We do not show the case where the vertical permeability exceeds the horizontal permeability as this is never observed in geological formations. Then the main conclusions for this study are presented.

2. Experimental Set-up

Figure 1 shows the schematic of the set-up used to carry out the experiments. It consists of two stainless steel vessels, the measurement vessel with inner diameter of $D_1=30mm$ and the gas storage vessel with the inner diameter of $D_2=40mm$. The length of both vessels is $10cm$. The vessels are sealed and kept at constant temperature of $T=30\pm 0.1^\circ C$ in an oven. The small vessel was filled with two types of sand grains (with an average diameter of $1.5mm$ and $0.7mm$) up to the desired height and then saturated with water at standard conditions. The porosity of both sand packs was measured to be $\varphi_1 = \varphi_2 = 0.40$. Using the Karman-Kozeny correlation the permeabilities were calculated to be $k_1 \approx 1850D$ and $k_2 \approx 400D$. CO₂ was slowly injected into the measurement vessel from the storage vessel. The gas pressure is measured with two calibrated pressure gauges, which are connected to the top of the vessels. When the CO₂ pressure reached the desired value, the valve connecting the vessel containing the porous medium was closed and the cell was isolated. This was the starting time of the experiment. The gas pressure was monitored and recorded every 100 seconds with the aid of a computer.

3. Physical model

If the fluid in the porous medium is in mechanical equilibrium in a gravitational field the concentration in the z direction will be merely a function of the distance from the interface, i.e., $c = c(z)$. Nevertheless, if the concentration varies in the x direction or if the vertical concentration gradient value exceeds a certain value, mechanical equilibrium is not possible and the fluid inside the porous medium starts to move to return the system to equilibrium [19]. We formulate the relevant natural convection/ diffusion equations.

We consider a porous medium saturated with a fluid with a height H and length L . In this paper we do not investigate the effect of aspect ratio, therefore we restricted the analysis to the situation where $H=L$. The porosity of the porous medium is denoted by φ . The ratio between the vertical permeability, k_v , and the horizontal permeability, k_h , is ϑ . In the case of two layered reservoir, each layer is assumed to be isotropic and homogeneous. We apply

no flow conditions at the bottom, left side and right side of the porous medium. Initially the fluid is at rest and there is no CO₂ dissolved in the fluid. CO₂ is continuously supplied from the top, i.e., CO₂ concentration at the top is kept constant. We assume that CO₂-liquid interface is relatively sharp and fixed. Moreover, we assume a no-flow boundary at the bottom of the porous medium. We assume that the porous medium is completely filled with water and hence there is no capillary transition zone between the gas and the liquid phase. Hence we only model the liquid phase and the presence of the gas phase at the top is represented by a boundary condition for the liquid phase. The motion of fluid is described by Darcy's law with a source term proportional to the density gradient. Darcy's law is combined with the mass conservation laws for the two components (CO₂ and either water or oil) to describe the diffusion and natural convection processes in the porous medium. We only expect a laminar regime since Rayleigh's number is low. The density gradient is the source of natural convection and therefore the density cannot be considered constant. However, we use Boussinesq approximation which considers density variations only when they contribute directly to the fluid motion.

3.1. Formulation

For the 2D porous medium shown in Fig. 2, the governing equations can be written as

(a) *Continuity Equation*

$$\phi \frac{\partial \rho}{\partial t} + \frac{\partial(\rho U_x)}{\partial X} + \frac{\partial(\rho U_z)}{\partial Z} = 0 \quad , \quad (1)$$

(b) *Darcy's law*

$$U_x = -\frac{k_h}{\mu} \frac{\partial p}{\partial X} \quad , \quad (2)$$

$$U_z = -\frac{k_v}{\mu} \left(\frac{\partial p}{\partial Z} - \rho g \right) \quad , \quad (3)$$

(c) *Concentration*

$$\frac{\partial c'}{\partial t} + U_x \frac{\partial c'}{\partial X} + U_z \frac{\partial c'}{\partial Z} = \phi D \left(\frac{\partial^2 c'}{\partial X^2} + \frac{\partial^2 c'}{\partial Z^2} \right). \quad (4)$$

The fluid becomes denser when CO₂ is present at the top part of the porous medium. We assume that the liquid density changes linearly with the increasing CO₂ concentration, i.e.,

$$\rho = \rho_0 [1 + \beta_c (c' - c'_0)] \quad , \quad (5)$$

from which we obtain

$$\frac{\partial \rho}{\partial X} = \rho_0 \beta \frac{\partial c'}{\partial X} \quad . \quad (6)$$

In Eqs. (1)-(4) we have four unknowns (U_x , U_z , p and c'). It is possible to eliminate the pressure by cross-differentiating Eqs. (2) and (3) (Eq. (2) with respect to Z and Eq. (3) with respect to X). This leads to

$$\frac{\partial U_z}{\partial X} - \frac{\partial U_x}{\partial Z} = \frac{k_g \rho_0 \beta}{\mu} \frac{\partial c'}{\partial X} \quad . \quad (7)$$

Therefore, the equations to be solved are Eqs. (1), (4) and (7) to obtain U_x , U_z and c'

3.2. Dimensionless form of the equations

We take H as characteristic length and define the following dimensionless variables

$$x = \frac{X}{H}, \quad z = \frac{Z}{H}, \quad u_x = \frac{H}{\phi D} U_x, \quad u_z = \frac{H}{\phi D} U_z, \quad \tau = \frac{D}{H^2} t, \quad c = \frac{c' - c'_i}{c'_0 - c'_i}$$

$$u_x = -\frac{\partial \psi}{\partial z}, \quad u_z = \frac{\partial \psi}{\partial x}, \quad \vartheta = \frac{k_v}{k_h}, \quad \text{Ra} = \frac{k_h \rho_0 \beta g H \Delta c'}{\phi D \mu} = \frac{\Delta \rho g k_h H}{\phi D \mu} \quad (8)$$

Thus, after applying the Boussinesq approximation the dimensionless form of the equations can be written as

$$\frac{1}{\vartheta} \frac{\partial^2 \psi}{\partial x^2} + \frac{\partial^2 \psi}{\partial z^2} = \text{Ra} \frac{\partial c}{\partial x} \quad , \quad (9)$$

$$\frac{\partial c}{\partial \tau} + \frac{\partial \psi}{\partial z} \frac{\partial c}{\partial x} - \frac{\partial \psi}{\partial x} \frac{\partial c}{\partial z} = \frac{\partial^2 c}{\partial x^2} + \frac{\partial^2 c}{\partial z^2} \quad (10)$$

3.3. Boundary and initial conditions

The initial condition of the problem is

$$\psi = 0, c = 0 \text{ at } \tau = 0 \quad (11)$$

The boundary conditions of the problem are

$$\begin{aligned} \psi = 0, \frac{\partial c}{\partial z} = 0 \text{ at } x = 0 \\ \psi = 0, c = 1 \text{ at } z = 0 \\ \psi = 0, \frac{\partial c}{\partial x} = 0 \text{ at } x = 1 \\ \psi = 0, \frac{\partial c}{\partial x} = 0 \text{ at } z = 1 \end{aligned} \quad (12)$$

A modified version of the numerical method explained by Guceri and Farouk [20] was applied to solve the system of equations (9) and (10), i.e., the finite volume approach. The details of solution procedure are explained in refs. [18,20].

4. Results and discussion

4.1. Experimental results

Figure 3 shows gas pressure versus time measured during CO₂ mass-transfer experiments where (a) a high permeable layer is overlain (Exp-01, P₀=46bar) or (b) underlain by a less permeable layer (Exp-02, P₀=43bar). In both cases gas pressure decreases with time due to the transfer of CO₂ molecules into water. The initially pressure declines is consist with a diffusion-controlled mass-transfer process,. However, after a certain time, the curve becomes steeper. This indicates the onset of density-driven convection that accelerates the mass transfer. The switching time is shorter for the case when the high permeable layer is on top which agrees well with the theory presented in Ref. 18. With a simple scaling analysis it is possible to evaluate the significance of natural convection. The time scale for CO₂ diffusion through a water layer with thickness of $L=7cm$ at our experimental condition is $t=L^2/D \approx 24 \times 10^5 sec \approx 680hr$, where $D=2 \times 10^{-9}$ is the diffusion coefficient of CO₂ into water. It can be seen from Fig. 3 that the time of dissolution of CO₂ into water is much shorter than the time predicted by Fick's law indicating that natural convection has a significant effect on transfer of CO₂ in porous layers. When the high permeable layer is on top (Exp-02) the system reaches equilibrium faster than for Exp-01.

In this stage we did not use the theory for the interpretation of the experiments, because (1) the theory is in Cartesian system coordinates, whereas the experiments are in cylindrical coordinates, which poses some difficult numerical problems and (2) the comparison would entail only a few experiments which can possibly lead to premature conclusions. Therefore, we leave the comparison between theory and experiments for future work. However, the comparison between the theory explained in Ref. 6 for the bulk experiments (CO₂ on top of a water layer) shows a reasonable match with the corresponding experiment [21]. Comparisons involving experiments in porous media still need to be made.

4.2. Simulation results

In this section we discuss simulation results for the system described in section 3. To observe the non-linear behavior, i.e., the fingering behavior it was necessary to disturb the interface. Therefore, a sinusoidal perturbation in the x -direction was imposed at the interface, i.e., $c(x, z = 0, t = 0) = 1 + A_0 \sin(2\pi x / \lambda)$, where $A_0 = 0.01$ and $\lambda = 1/12$. All simulations use 81×81 grid cells in Matlab.

Our numerical calculations are confined to situations where a high permeable aquifer is either overlain or underlain by a less permeable layer. To investigate the effect of natural

convection in a dual layered porous medium two different situations are considered. In the first case the Rayleigh number in the bottom layer is 500 (subject to convection) and in the top layer is 40 (no convection). Moreover we investigate the effect of anisotropy by varying the permeability ratio ϑ for values of 1, 0.5, and 0.1. We ignore any irregularities at the interface between the two layers; however it must be pointed out that such irregularities can significantly affect the flow by disturbing the interface and therefore cause additional fingering.

4.2.1. Case 1: $Ra_1=500, 1000, 2000$ and $Ra_2=40$

Figure 4 shows the concentration profile for the aquifer ($Ra_1=500$) on top of the low permeable layer ($Ra_2=40$). At early times ($\tau=7 \times 10^{-3}$) the behavior is diffusion like, without any observable natural convection effects. For times beyond $\tau=7 \times 10^{-3}$ natural convection effects become visible. The natural convection effects increase until the $c=0.1$ contour hits the low permeable layer ($\tau=1.4 \times 10^{-2}$). The natural convection effects damp out and fingers disappear in the low permeable layer. The results of the flow in top layer are similar to the homogenous case with the aspect ratio of 2 [18]. Figure 5 shows the advance of the average position of the $c=0.1$ contour as a function of the logarithm of time. Indeed initially we observe the square root of time behavior that is characteristic of a diffusion process. Then the behavior becomes dominated by natural convection effects and shows more linear behavior with time. As the $c=0.1$ contour hits the low permeable later the convection effects decrease, however; the behavior does not become diffusion alone since the slope is larger than 0.5. Moreover the stream function profile shows that there is a non-zero velocity although its magnitude is smaller than the upper layer. A similar behavior is observed when the Rayleigh numbers are increased to 1000 and 2000 respectively. However the times at which the switching happens decreases with increasing Rayleigh number.

4.2.2. Case 2: $Ra_1=40, Ra_2=500, 1000, 2000$

Figure 6 shows the results for the aquifer ($Ra_1=500$) below the low permeable layer ($Ra_2=40$). The behavior remains diffusion like during the times that the $c=0.1$ contour stays above the aquifer. The diffusion like behavior continues as the contours penetrate the aquifer. This is similar to the behavior that we reported in previous paper on homogeneous reservoirs and in case 1. When the contours have penetrated appreciably in the aquifer, natural convection like behavior starts to occur. The natural convection effects increase with time and start even to affect the low permeable layer on top. This is a striking result as natural convection effects are not expected to occur in the low permeable region. A plot like Fig. 5 shows that initially there is diffusion like behavior for all Rayleigh numbers considered. At the onset of natural convection behavior the advance of the contour grows linearly with time. Again this time decreases with increasing Rayleigh number. The initial perturbation does not affect the final results, (it is dampened in the low permeable layer).

4.2.3. Case 3: Effect of anisotropy

Anisotropy in this paper is only considered for permeability and not for the diffusion coefficient. In general the reduction of the vertical permeability suppresses the convection effects. This means that an increase in the vertical permeability increases the critical Rayleigh number and decreases the critical time (Fig. 7) for the onset of convection.

From numerical results it is observed that the wavelength to initiate convection effects increases with decreasing permeability ratio, i.e., ϑ (Fig. 8, for details see ref. [18]). This is in agreement with the analytical analysis of Ennis-King et al [17].

5. Conclusions

We have investigated natural convection effects in porous media experimentally by following the pressure decline in a column of gas on top of a porous medium. When the low permeable layer is on top, initially diffusion like behavior occurs, but after some time the natural convection enhanced transfer between the gas layer and the porous medium occurs. When the low permeable layer is at the bottom, natural convection starts almost immediately, but decreases in strength when the carbon dioxide penetrates in the low permeable layer. The

dissolution rate is faster with the high permeable layer on top; this is in qualitative agreement with the numerical analysis shown above.

We investigated the effect of natural convection in a dual layered and anisotropic porous media also numerically. It was shown that when the aquifer is overlain or underlain by a less permeable layer natural convection dominates the flow. In agreement with the theory we observe that a high layer on top is more favorable for fast transfer, but also with the low permeable layer on top natural convection effects occur.

The reduction in vertical permeability reduces the convection effects. The wave-number for fastest growing fingers decreases with increasing anisotropy

6. References

1. Lindeberg E., Wessel-Berg D., *Energy Convers. Manage.*, 38, S229-S234 (1997)
2. Gmelin L., *Gmelin Handbuch der anorganischen Chemie*, 8. Auflage. Kohlenstoff, Teil C3, Verbindungen., pp 64-75 (1973).
3. Ashcroft S. and Ben Isa M., *J. Chem. Eng. Data*, 1244-1248 (1997).
4. Yang Ch., Gu Y., *Ind. Eng. Chem. Res.*, 45, 2430-2436 (2006).
5. Farajzadeh R, Barati A., Delil H.A., Bruining J., Zitha P.L.J., 25, Issue 12, 1493-1511 (2007).
6. Farajzadeh R, Delil H.A., Zitha P.L.J., Bruining J., SPE 107380 (2007).
7. Castinel G. and Combarnous M., *Int. Chem. Eng.* 17, 605 (1977).
8. McKibbin, in *Convective Flows in Porous Media*, edited by R. A. Wooding and I. White DSIR Science Information, Wellington, New Zealand, 1985, pp. 113–127.
9. Kimura Sh and Okajima A, *Heat Transfer, Asian Research*, 29(5), (2000)
10. Kvernfold O and Tyvand PA, *J. Fluid Mech.* 90, 609 (1979).
11. Epherre F, *Int. Chem. Eng.* 17, 615 (1977).
12. McKibben R and Tyvand, *J. Fluid Mech.* 118, 315-339 (1982).
13. McKibben R and O'Sullivan, *J. Fluid Mech.* 96, 375-393 (1980).
14. Leong JC and Lai FC, *Journal of Thermophysics and Heat Transfer*, 18, 4, (2004).
15. Degan G, Vasseur P, Bilgen E, *Int. J. Heat Mass Transfer*, 38, 11 (1995).
16. Vasseur P. and Wang CH., *Chem. Eng. Comm*, 114, 145-167 (1992).
17. Ennis-King J., Preston I. and Paterson L., *Physics of Fluids*, 17, 84107 (2005).
18. Farajzadeh R, Salimi H., Zitha P.L.J., Bruining J., *Int. J. Mass Heat Trans.*, 50, 5054-5064 (2007).
19. Landau L.D. and Lifshitz E.M., *Fluid mechanics, Volume 6 of course of theoretical physics*, translated from Russian by Sykes J.B. and Reid W.H., pp. 212-218, 4th Edition, Pergamon Press, 1975.
20. Guçeri S. and Farouk B., *Numerical solutions in laminar and turbulent natural convection*, In: Natural convection, Fundamentals and applications, S. Kakac, W. Aung, R. Viskanta, Hemisphere publication, 615-655 (1985).
21. Farajzadeh R, Zitha PLJ, Bruining J, to be submitted (2008).

FIGURES

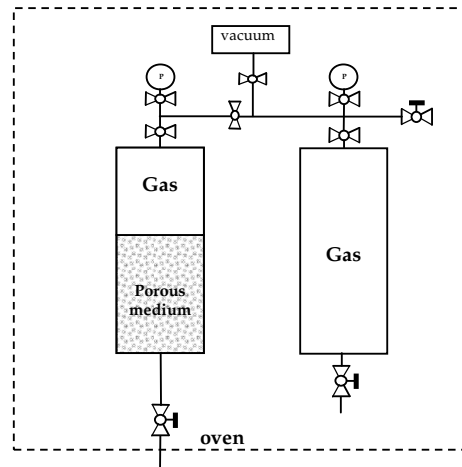


Fig. 1: Schematic of the experimental set-up

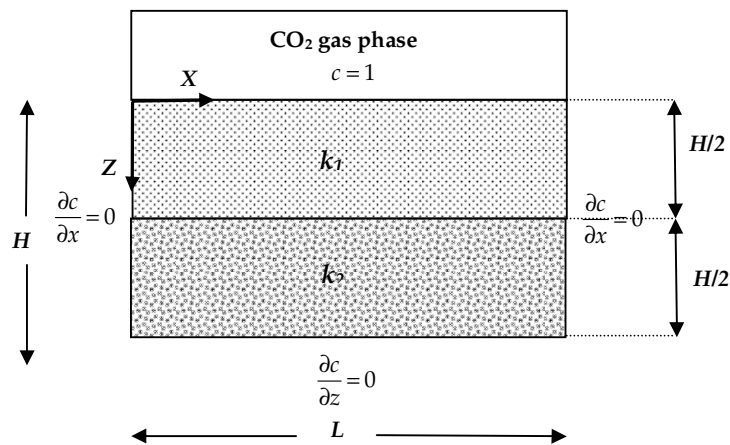


Fig. 2: Schematic of the dual layered porous medium and coordinates

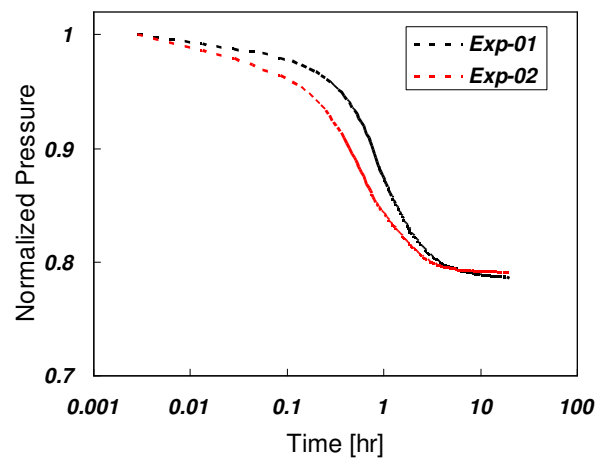


Fig. 3: Experimental pressure decline versus square-root of time

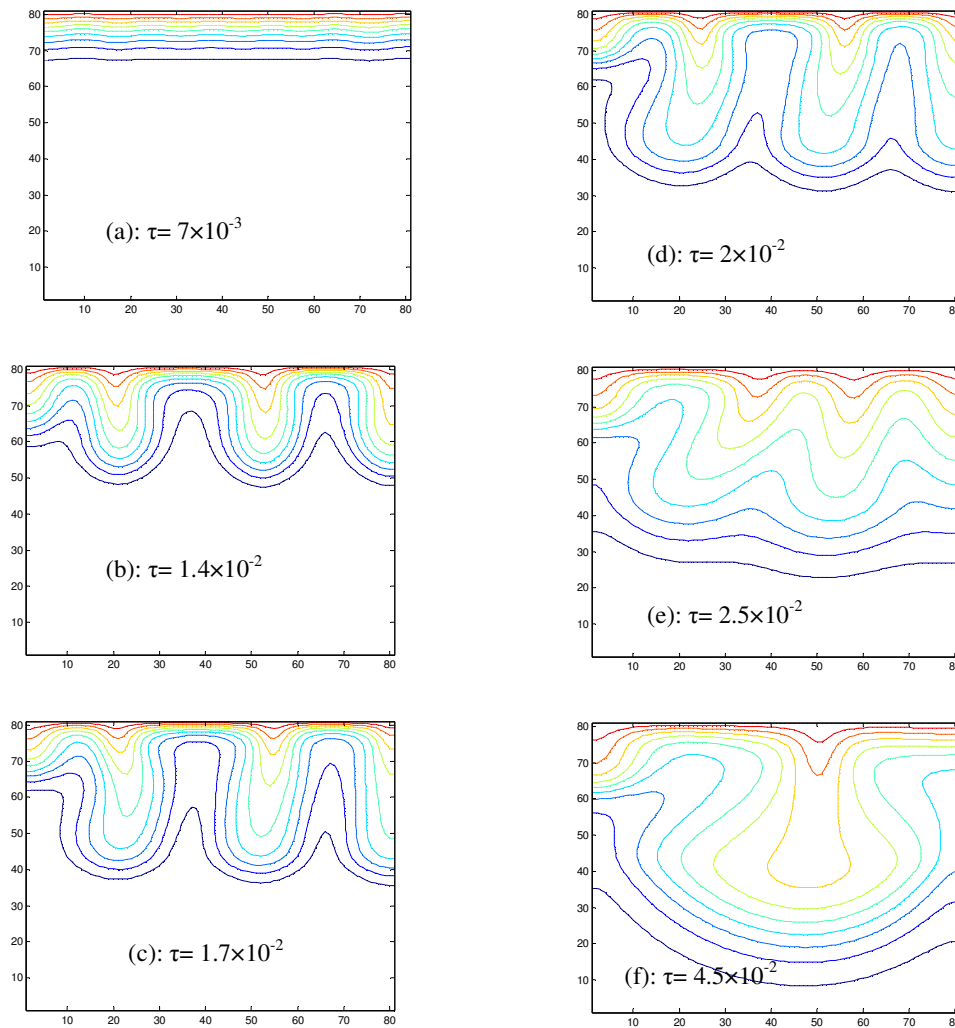


Fig. 4: concentration profiles for $Ra_1=500$ and $Ra_2=40$ at $\tau =$ (a) 7×10^{-3} , (b) 1.4×10^{-2} , (c) 1.7×10^{-2} , (d) 2×10^{-2} , (e) 2.5×10^{-2} , (f) 4.5×10^{-2} .

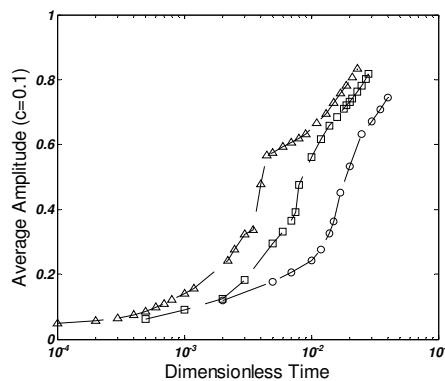


Fig. 5: Progress of the tip of $c=0.1$ contour for different Rayleigh numbers as a function time

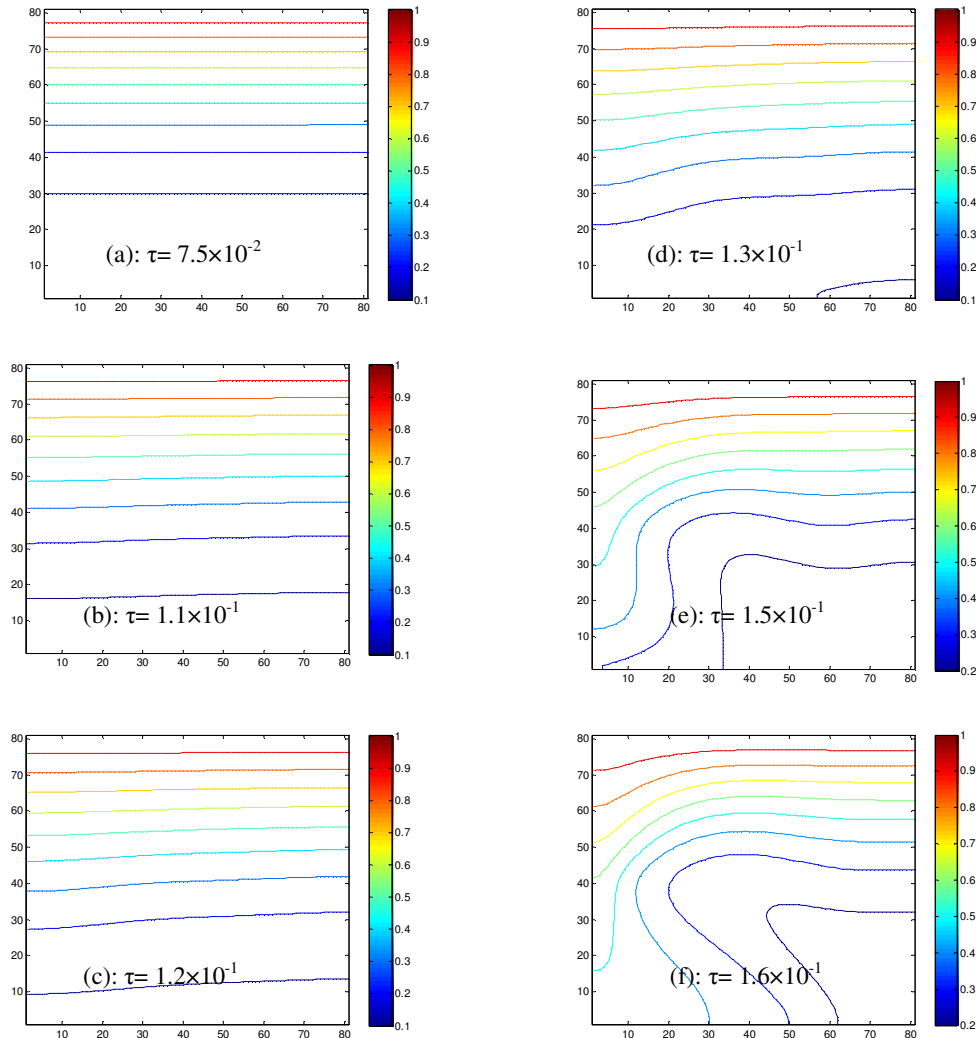


Fig. 6: concentration profiles for $Ra_1=40$ and $Ra_2=500$ at $\tau=$ (a) 7.5×10^{-2} , (b) 1.1×10^{-1} , (c) 1.2×10^{-1} , (d) 1.3×10^{-1} , (e) 1.5×10^{-1} , (f) 1.6×10^{-1}

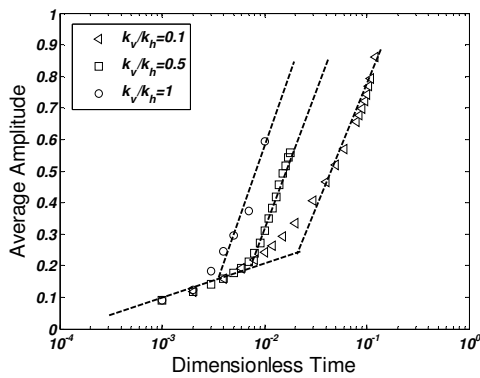


Fig. 7: Front move for different permeability ratios

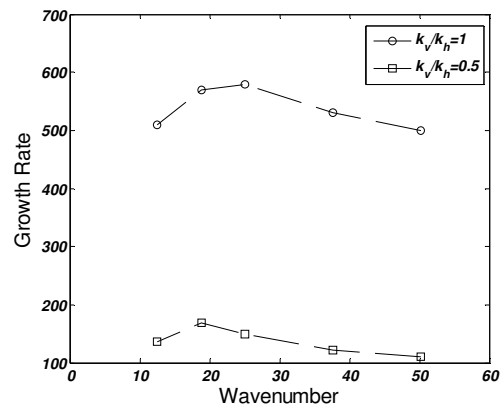


Fig. 8: Growth rate coefficient as a function of wave-number for $Ra=1000$